UC Irvine
UC Irvine Previously Published Works

Title
STRESS TRANSIENTS GENERATED BY EXCIMER-LASER IRRADIATION OF POLYIMIDE

Permalink
https://escholarship.org/uc/item/3xn5z5cg

Authors
ZWEIG, AD
VENUGOPALAN, V
DEUTSCH, TF

Publication Date
1993

Copyright Information
This work is made available under the terms of a Creative Commons Attribution License, availalbe at https://creativecommons.org/licenses/by/4.0/

Peer reviewed

eScholarship.org Powered by the California Digital Library
University of California

STRESS TRANSIENTS GENERATED BY EXCIMER-LASER IRRADIATION OF POLYIMIDE

A. D. ZWEIG*, V. VENUGOPALAN*†, and T. F. DEUTSCH*
* Wellman Laboratories of Photomedicine, Massachusetts General Hospital, Department of Dermatology, Harvard Medical School, Boston, MA 02114.
† Department of Mechanical Engineering, Massachusetts Institute of Technology, Cambridge, MA 02139.

ABSTRACT

We measure the stress transients resulting from pulsed excimer laser irradiation of polyimide at 351, 308, 248 and 193 nm, using thin (9 μm) piezoelectric PVDF (polyvinylidene fluoride) films. We find that fluences between $3 \cdot 10^{-3}$ and 10^2 J/cm^2 generate peak stresses between 10^4 and 10^9 Pa. Further, the results show three ranges of fluence where different physical mechanisms mediate the stress generation. In the lowest range of fluence, subsurface thermal decomposition (for λ = 351 and 308 nm) and photodecomposition (for λ = 248 and 193 nm) govern the generation of the observed stresses. At higher fluences we identify two regimes, independent of laser wavelength, where the gas dynamic expansion of the ablation products and plasma formation and expansion, are responsible for the generated stresses.

Introduction

Excimer-laser ablation of solids has become an important topic in microelectronics and surgery for the photoetching and submicron patterning of organic polymers (e.g., polyimide, PMMA, PET, etc.) and for the incision and excision of biological tissue [1, 2]. In a typical application, the laser energy is deposited in nanoseconds and results in the development of substantial stresses ($\sim 10^5$ Pa) which have the potential to produce functional and morphological damage in tissue [3, 4]. In this study, we measure and characterize the stresses induced by pulsed excimer-laser irradiation of polyimide in order to understand the physical mechanisms which govern the generation of these stresses and the dynamics of the ablation process.

Materials and Methods

We measure the stress transients resulting from excimer laser irradiation of 125μm-thick sheet polyimide at 351, 308, 248 and 193 nm, using an experimental setup similar to that described in [5]. The electrical output of the transducer is taken via a series 50-Ω matching resistor and a coaxial cable into the 1-MΩ plug-in of a digital storage oscilloscope (Tektronix 7834, 200 MHz bandwidth) or digitizer (Tektronix AD 7912, 750 MHz bandwidth). In this case the output voltage of the transducer is described by the relation [6]:

$$V(t) = \frac{e_{33}}{C_D + C_L} A\bar{\sigma}(t), \tag{1}$$

where $e_{33} = -33$ pC/N is the piezoelectric stress constant of the PVDF film, A is the surface area of the irradiated spot and $\bar{\sigma}(t)$ is the time varying average stress in the PVDF film. $C_D \approx 6.3$ nF and C_L are the capacitances of the transducer and the load, respectively. The temporal response of the transducer is limited by the propagation time of a stress wave across the PVDF film, $\approx$4 ns.

A Lambda Physik EMG 103/MSC excimer laser (XeF, XeCl, KrF or ArF) was the source of UV radiation. The laser emits pulses with a full width at half maximum duration between 18 and 24 ns, depending on wavelength. Using an 8-mm aperture, we select a uniform portion of the laser beam. This portion of the beam propagates through a set of attenuators, a beam splitter, a 160-mm focal length lens to a prism which deflects the laser output onto the target surface. The radiant energy incident on the target surface is determined by measuring the energy in the split off part of the beam using a pyroelectric detector (Molectron J3-09) and correcting for the optical losses. For a given wavelength, we took data in a range spanning over 4 decades of fluence.

Mat. Res. Soc. Symp. Proc. Vol. 285. ©1993 Materials Research Society

Downloaded from https://www.cambridge.org/core. Access paid by the UC Irvine Libraries, on 31 Oct 2018 at 20:28:15, subject to the Cambridge Core terms of use, available at https://www.cambridge.org/core/terms. https://doi.org/10.1557/PROC-285-69

Results

Figures 1a and 1b show measured stress transients resulting from 308-nm irradiation of polyimide below (1a) and above (1b) the threshold for ablation. The compressive stress transient rises to its maximum value in a time approximately equal to the laser pulse duration and returns to baseline only after a few hundred nanoseconds. At low fluences, this is followed by a tensile stress whose peak amplitude is less than 10 % of the peak compressive stress. At higher fluences, no tensile stress is observed. The successive maxima are due to acoustic reflections in the system. The separation between these maxima is given by twice the transit time of an acoustic wave across the thickness of the sample.

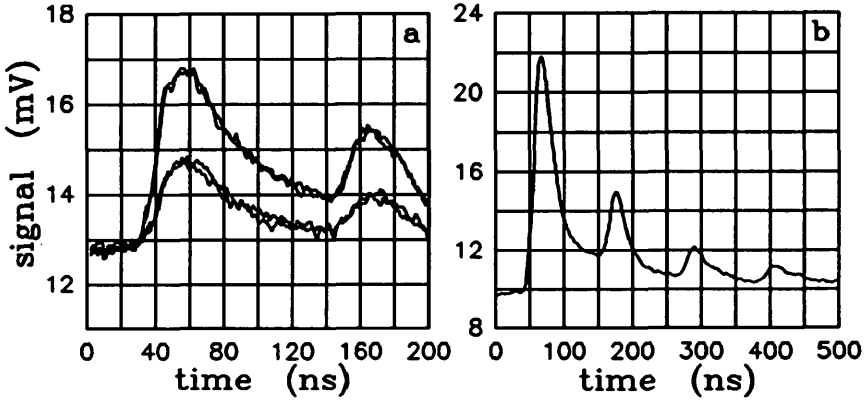

Figure 1: Sample traces of stress transients as measured by the stress transducer. These transients result from 308-nm irradiation of polyimide. **(a):** The incident fluences for the top and bottom traces are F= 0.034 and 0.018 J/cm^2, respectively. The sensitivity of the detector is 20 kPa/mV. **(b):** The incident fluence is 0.062 J/cm^2 and the detector sensitivity 27 kPa/mV.

Figures 2a and 2b are plots of the peak laser-induced stress, σ_p, versus fluence, F, at the four wavelengths tested. For low fluences, the peak laser-induced stress is proportional to $F^{1.5}$ when λ = 193 or 248 nm and proportional to F when λ = 308 or 351 nm. As the fluence increases, a threshold is passed above which the maximum laser-induced stress increases abruptly with further increase in the fluence. At higher fluences the maximum laser-induced stress is proportional to $F^{3/4}$. Figures 3a and 3b show the mechanical coupling coefficient, C_m, versus the average irradiance of the laser pulse, I. The mechanical coupling coefficient is defined as $\int_0^\infty \sigma(t)\,dt/F$ and is approximated by σ_p/I. This gives a measure of the degree to which the laser energy is converted to mechanical impulse.

Discussion

Stress Generation at Low Fluences

At low fluences, 351 and 308-nm irradiation of polyimide results in peak stresses which scale linearly with the laser fluence. This behavior is often associated with the thermoelastic effect. In our experiments, the laser pulse duration is always much longer than the acoustic transit time across the optical penetration depth in the sample. The optical penetration depths of excimer laser radiation in polyimide range from $1/\mu_a$ = 24 nm at λ = 193 nm to $1/\mu_a$ = 384 nm at λ = 351 nm. In this limiting case, waveforms characteristic of thermoelastic behavior have a duration equal to the laser pulse duration and a peak amplitude proportional to the laser fluence *independent* of optical absorption coefficient [7]. From figures 1a and 2b it is clear that our measured stress transients do not satisfy either of these criteria. First, the waveform shown in figure 1a has a duration of $\approx$ 100 ns, much longer than the laser pulse duration. Second, fig-

Downloaded from https://www.cambridge.org/core. Access paid by the UC Irvine Libraries, on 31 Oct 2018 at 20:28:15, subject to the Cambridge Core terms of use, available at https://www.cambridge.org/core/terms. https://doi.org/10.1557/PROC-285-69

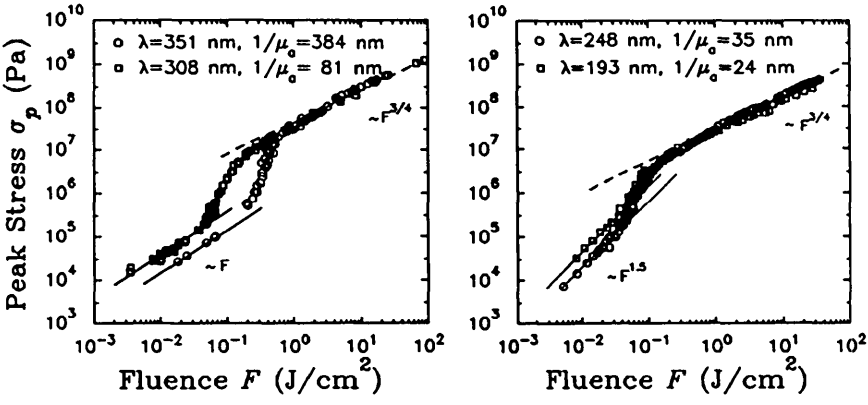

Figure 2: Peak stress, σ_p, generated by excimer laser irradiation of polyimide vs. fluence, F, for different wavelengths λ. (a): λ = 351 nm, (o) and λ = 308 nm, (□); (b): λ = 248 nm, (o) and λ = 193 nm, (□).

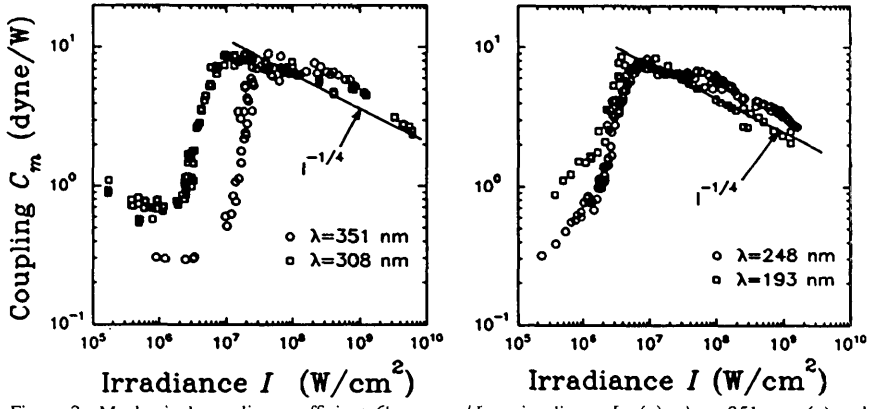

Figure 3: Mechanical coupling coefficient $C_m \approx \sigma_p/I$ vs. irradiance I. (a): λ = 351 nm, (o) and λ = 308 nm, (□); (b): λ = 248 nm, (o) and λ = 193 nm, (□).

ure 2b shows that for a given fluence, the peak stress is not equal for the two laser wavelengths. Thus the observed stresses in this fluence regime are not produced by the thermoelastic effect.

We believe that the observed stresses are due to expansion of gas produced by thermal decomposition during the laser pulse. The deposition of laser energy causes a rise in pressure in the gas and generates a compressive stress transient which reaches a maximum at the end of the laser pulse. After the end of the laser pulse, the pressure in the gas drops due to deformation of the target, cooling of the gas, and diffusion of the gas out of the target. This hypothesis is consistent with studies of laser-induced fluorescence which have detected the release of C_2 and CN from polymer surfaces when subjected to UV radiation at fluences below the ablation threshold [8]. If this is the case, the pressure generated in the gas should scale with the volumetric energy deposition, $\mu_a F$, when thermal diffusion is absent. Thus for a given laser fluence, the peak stresses should scale according to the ratio of the optical absorption coefficient. In fact, the peak stresses generated at 308 nm are $\approx$ 2.7 times larger than those generated at 351 nm while the ratio of the optical absorption coefficients is $\approx$ 4.7. This difference is due to thermal diffusion since the laser pulse duration is much larger than the characteristic thermal diffusion time across the optical penetration depth.

For irradiation at 248 and 193 nm, the peak stresses are not proportional to the laser fluence but instead

Downloaded from https://www.cambridge.org/core. Access paid by the UC Irvine Libraries, on 31 Oct 2018 at 20:28:15, subject to the Cambridge Core terms of use, available at https://www.cambridge.org/core/terms. https://doi.org/10.1557/PROC-285-69

$\propto F^{1.5}$. Thus it is likely that the mechanism for stress generation at these wavelengths is different from that proposed above. While we are not certain as to what the responsible mechanism is, it may be related to the process of ablative photodecomposition which is thought to mediate the laser-polymer interaction at these photon energies.

Stress Generation due to Recoil of Ablation Products

At larger fluences, material removal occurs and the stress transients are dominated by the recoil of the ablation products. As such the peak stress is no longer controlled by the laser wavelength or the optical absorption coefficient but by parameters which govern the gaseous expansion of the ablation products. The onset of this regime is reflected in the change in slope of the σ_p vs. F curves shown in figures 2a and 2b. The recoil stress at the target surface is equal to the pressure in the ablative flow. This pressure can be estimated using a simple model which considers the one-dimensional expansion of a fixed mass of ideal gas which is heated by a laser pulse and enclosed on either side with a piston of acoustic impedance $Z_i = \rho_i c_i$ [9] where ρ_i and c_i are the density and speed of sound in the piston materials. The model assumes that the rapid heating of the gas results in the development of shock waves in both the confining pistons. Thus the piston surfaces travel at the particle velocity characteristic of the passage of the shock through the piston material. This leads to the following scaling between the maximum pressure in the gas, p_{max}, and the laser and gas parameters:

$$p_{max} \propto \left[\frac{Z\,(F - F_0)}{t_p\,(1 + f/2)}\right]^{1/2} \tag{2}$$

where $Z = Z_1 Z_2/(Z_1 + Z_2)$, t_p the laser pulse duration, F_0 the residual energy left in the target and $f = 2c_v/R$ for the gaseous ablation products, c_v being the specific heat and constant volume and R the universal gas constant. In our case, Z_1 is the acoustic impedance of polyimide, = 3.1 MPa s/m and Z_2 is that of the confining medium, air, which is given by $Z_2 = [(\gamma + 1)\,p/(2\rho_{air})]^{1/2}$, where γ is the ratio of specific heats, (c_p/c_v), for air. For pressures less than $\approx$1 TPa, $Z_1 \gg Z_2$ and thus $Z \approx Z_2$. This leads to the following scaling law for the maximum pressure in the ablative flow:

$$p_{max} \propto \left[\frac{(\gamma + 1)\rho_{air}}{2}\right]^{1/3} \left[\frac{1}{1 + f/2}\right]^{2/3} \left[\frac{(F - F_0)}{t_p}\right]^{2/3} \tag{3}$$

Importance of Thermal Diffusion

Figure 4 is a plot of σ_p vs. F for 308-nm laser irradiation of polyimide in this regime. This figure also presents data from 193-nm laser ablation of cornea [10] which has a threshold fluence for ablation virtually identical to that of 308-nm laser ablation of polyimide. We also present a best fit of this data to a $(F - F_0)^{2/3}$ scaling with $F_0 = 0.048$ J/cm^2. This scaling law appears to be valid for the stresses generated by 193-nm laser ablation of cornea while it fails to describe those generated by 308-nm laser ablation of polyimide. This failure is due to thermal diffusion which contributes substantially to the transport of energy in the polyimide target, but not in cornea.

In the absence of material removal, thermal diffusion results in the transport of energy over a time t to a depth $\delta \propto (\alpha t)^{1/2}$ where α is the thermal diffusivity of the medium, 7.75 and 14.4 $\cdot$ (10^{-4}cm^2/s) for polyimide and water respectively. For a laser pulse duration of $\approx$ 20 ns, we find that δ is comparable to the penetration depth of 308-nm radiation in polyimide while it is more than 20 times smaller than the optical penetration depth of 193-nm radiation in cornea. Once material removal ensues δ is the larger of $(1/\mu_a)$ and (α/v_{abl}) where μ_a is the optical absorption coefficient of the incident radiation and v_{abl} is the speed at which the target surface recedes during material removal [11, 12]. The Péclèt number, $\mathrm{Pe} = v_{abl}/\alpha\mu_a$, is the parameter which indicates if thermal diffusion ($\mathrm{Pe} \lesssim 1$) or the movement of the ablation front ($\mathrm{Pe} \gtrsim 1$) governs the distribution of energy in the bulk of the target [12]. Furthermore, one can also show that for a steady ablation process, the fraction of deposited laser energy lost into the target via diffusion is given by the quantity $1/(1 + \mathrm{Pe})$ [12].

Downloaded from https://www.cambridge.org/core. Access paid by the UC Irvine Libraries, on 31 Oct 2018 at 20:28:15, subject to the Cambridge Core terms of use, available at https://www.cambridge.org/core/terms. https://doi.org/10.1557/PROC-285-69

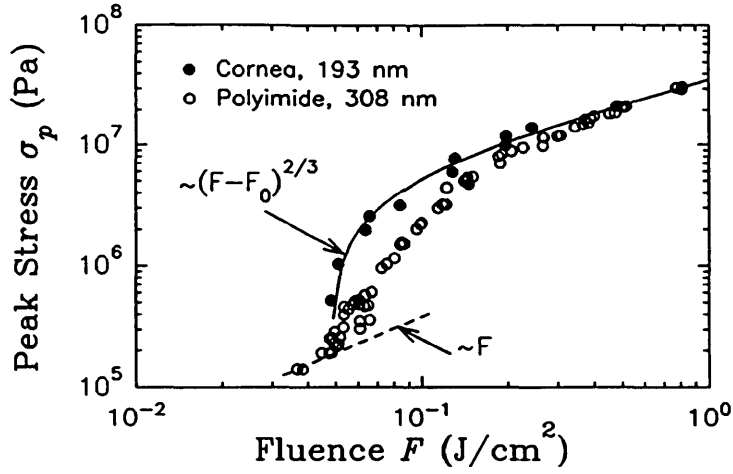

Figure 4: Peak stress, σ_p vs. fluence, F in the regime where recoil of the ablation products dominates the stress generation. Data is shown for 308-nm laser ablation of polyimide (o) and 193 nm laser ablation of cornea (•) [9]. The cornea data is well described by the $\sigma_p \propto (F - F_0)^{2/3}$ scaling law where F_0 = 0.48J/cm^2. The deviation of the polyimide data from this scaling law is due to thermal diffusion (see text).

If we assume a blow-off model is accurate in predicting the depth to which a polymer is etched, we can approximate the Péclèt number by $\mathrm{Pe} = \ln(F/F_0)/(t_p \alpha \mu_a \mu_{eff})$ where μ_{eff} is the slope of the etch depth vs. log F characteristic. Doing this we find that at $F = 1.5F_0$, Pe = 32.4 and 3.6 for cornea and polyimide, respectively. Thus the rate at which energy is lost via diffusion into the target during the ablation process is a mere 3 % of the irradiance absorbed by the target for 193-nm laser ablation of cornea but 22 % for 308-nm laser ablation of polyimide. In fact, we can estimate this energy loss directly from Figure 3. We do this by calculating from eqn. (3) the fluence which corresponds to an experimentally measured stress. We then compare this calculated value with the actual laser fluence absorbed by the target to generate the measured stress. The difference is the amount of energy lost to thermal diffusion into the bulk. At a fluence of $F = 1.5F_0$, the energy lost into the target is ≈ 20 % of the absorbed fluence. As the fluence increases, this value decreases as the larger etch depths result in an increase in the Péclèt number and a reduction in the energy lost via thermal diffusion.

Stress Generation due to Plasma Formation and Expansion

At higher irradiances, a dense plasma is ignited in the ablation plume close to the target surface. After a time interval on the order of picoseconds, the plasma becomes self regulating; absorbing a constant fraction of the incident radiation and mediating the laser-target interaction. The threshold fluence for dense plasma formation is roughly coincident with the fluence at which the mechanical coefficient reaches a maximum [13]. Models which consider the absorption characteristics of the plasma as well as the gas dynamics of the expanding plasma and the ablation products predict the following scaling between the maximum pressure of the ablative flow, p_{max}, the mechanical coupling coefficient, C_m, and the laser parameters [13]:

$$p_{max} \propto F^{3/4} \lambda^{-1/4} t_p^{-7/8} \tag{4}$$

$$C_m \propto I^{3/4} \lambda^{-1/4} t_p^{-1/8} \tag{5}$$

We find that the data presented in Figures 2a and 2b follow this behavior and are indicative of a plasma-mediated ablation process.

Downloaded from https://www.cambridge.org/core. Access paid by the UC Irvine Libraries, on 31 Oct 2018 at 20:28:15, subject to the Cambridge Core terms of use, available at https://www.cambridge.org/core/terms. https://doi.org/10.1557/PROC-285-69

Conclusions

We have measured the stresses resulting from excimer laser irradiation of polyimide at $\lambda = 351, 308, 248$ and 193 nm at fluences between $3 \cdot 10^{-3}$ and 10^2 J/cm^2. For low fluences the mechanism responsible for the observed stresses is wavelength dependent. At 351 and 308 nm, the observed stresses are inconsistent with a thermoelastic mechanism of stress generation and are attributed to subsurface thermal decomposition of the polymer. At 248 and 193 nm, the stresses are caused by a different mechanism as the peak stresses scale as $F^{1.5}$. At higher fluences, the measured stresses are dominated by recoil of the ablation products. A model describing the gas dynamics of this process predicts that the peak stress scales as $(F - F_0)^{2/3}$. Finally, once the mechanical coupling coefficient has reached a maximum, the laser-target interaction is governed by plasma formation and expansion which permits a scaling of the peak stress, σ_p, with $F^{3/4}$.

Acknowledgement

We thank D. Rosen and D. Ferguson for their help with the assembly of the PVDF transducer system and J. Fujimoto for the loan of the Tektronix digitizer. We thank B. Braren for the supply of the sheet polyimide. ADZ is supported with grants from the Swiss National Science Foundation and the Air Force Office of Scientific Research. VV is supported by the Medical Free Electron Laser Program of the Department of Defense under Office of Naval Research grant N00014-91-C-0084.

REFERENCES

1. R. Srinivasan and B. Braren, Chem. Rev. **89**, 1303 (1989).
2. S. Trokel, J. Cataract Refract. Surg. **15**, 373 (1989).
3. Y. Yashima, D. J. McAuliffe, S. L. Jaques, and T. J. Flotte, Lasers Surg. Med. **11**, 62 (1991).
4. A. G. Doukas, D. J. McAuliffe, and T. J. Flotte, Ultrasound in Med. and Biol. (To appear).
5. P. E. Dyer and R. Srinivasan, Appl. Phys. Lett. **48**, 445 (1986).
6. H. Schoeffmann, H. Schmidt-Kloiber, and E. Reichel, J. Appl. Phys. **63**, 46 (1988).
7. J. C. Bushnell and D. J. McCloskey, J. Appl. Phys. **39**, 5541 (1968).
8. R. Srinivasan, Science **234**, 559 (1986).
9. R. D. Griffin, B. L. Justus, A. J. Campillo, and L. S. Goldberg, J. Appl. Phys. **59**, 1968 (1986).
10. P. E. Dyer and R. K. Al-Dhahir, SPIE Laser-Tissue Interaction **1202**, 46 (1990).
11. A. D. Zweig, J. Appl. Phys. **70**, 1684 (1991).
12. V. Venugopalan, N. S. Nishioka, and B. B. Mikić, ASME J. Biomech. Eng. (To appear).
13. C. R. Phipps Jr. et al., J. Appl. Phys. **64**, 1083 (1988).

Downloaded from https://www.cambridge.org/core. Access paid by the UC Irvine Libraries, on 31 Oct 2018 at 20:28:15, subject to the Cambridge Core terms of use, available at https://www.cambridge.org/core/terms. https://doi.org/10.1557/PROC-285-69